Eur Biophys J (1995) 24: 69–76

European Biophysics Journal

Pores formed in lipid bilayers and in native membranes by nodularin, a cyanobacterial toxin

M. Spassova[1], I. R. Mellor[2], A. G. Petrov[1], K. A. Beattie[3], G. A. Codd[3], H. Vais[2], P. N. R. Usherwood[2]

[1] Biomolecular Layers Department, Institute of Solid State Physics, Bulgarian Academy of Sciences, 72 Tzarigradsko Chaussee, BG-1784 Sofia, Bulgaria
[2] Department of Life Science, Nottingham University, University Park, Nottingham NG7 2RD, UK
[3] Department of Biological Sciences, University of Dundee, Dundee DD1 4HN, UK

Received: 28 March 1994 / Accepted in revised form: 9 January 1995

Abstract. Nodularin (NODLN), a cyclic pentapeptide hepatotoxin from the cyanobacterium *Nodularia spumigena*, induces pores in bilayers of diphytanoyl lecithin (DPhL) and in locust muscle membrane. NODLN increases the surface pressure of a DPhL monolayer; except when the surface pressure of the monolayer is high when the toxin causes a reduction of this parameter. NODLN pores exhibit many open conductance states; the higher state probabilities increasing when the transmembrane pressure is increased. The results from these studies are discussed in terms of two models for a NODLN pore, a torroidal model and a barrel-stave model. The edge energy of the NODLN pore of 1.4×10^{-12} J/m is determined.

Key words: Patch-clamp – Lipid monolayers – Lipid bilayers – Locust muscle membranes – *Nodularia spumigena* – Cyanobacterial toxins – Nodularin – Membrane pores – Edge energy

1. Introduction

Nodularin (NODLN, M.Wt. 824 Da), a cyclic pentapeptide found in the cyanobacterium (blue – green alga) *Nodularia spumigena*, is potently hepatotoxic (Carmichael 1989). Its sequence contains three unusual amino acids, namely N-methyl-dehydrobutyrine, β-methylaspartate and 3-amino-9-methoxy-2,6,8-trimethyl-10-phenyldeca-4,6-dienoic acid (ADDA), together with glutamic acid and arginine (Fig. 1 A–C). Glutamic acid and β-methylaspartic acid are negatively charged and arginine is positively charged at neutral pH, thus leaving one net negative charge per toxin molecule. On closer inspection of the space-filling model (Fig. 1 B, C) it appears that there is insufficient space in the centre of the NODLN cycle to accomodate a cation. The space seems to be filled by the free α-COOH group of β-methylaspartate. Thus, the familiar mode of ion channel-forming action of cyclic peptides seems less likely with NODLN.

NODLN is structurally similar to microcystin-LR (MCYST-LR), a cyclic heptapeptide found in cyanobacteria (Carmichael 1989). Like MCYST-LR, NODLN resembles a polar lipid, with the ADDA sidechain playing the role of a hydrophobic tail (see Fig. 2 in Petrov et al. 1991). MCYST-LR forms ionic pores in lipid bilayers (Petrov et al. 1991), possibly with its hydrophilic, cyclic moiety acting as a polar head group lining the inner surface of a pore (Fig. 2 A). The pore-forming property of MCYST-LR has been related to its wedge-like steric asymmetry (after Petrov et al. 1980, Petrov and Derzhanski 1987; Petrov 1988).

NODLN also features steric asymmetry of wedge-like type: it is emphasized in Fig. 1 B by dotted lines. The rigorous definition of wedge-like asymmetry of a biphilic molecule (Petrov et al. 1980) is based on the area difference between its hydrophilic head and hydrophobic tail cross-sections. This difference in the case of NODLN is also underlined in Fig. 1 C: the ADDA cross sectional area (shaded) is about 3 times less than the area of the hydrophilic cyclic region.

NODLN contains two fewer amino acids than MYCST-LR in its cyclic moiety (Fig. 1), therefore its steric asymmetry is weaker. Thus, in principle, more NODLN monomers would be necessary to create a membrane pore (Fig. 2 B). However, differences in the biphilic asymmetries of these two toxins may also influence their pore-forming potentials. In this paper we report on the surfactant and pore-forming properties of NODLN and show that this toxin forms pores in natural and artificial membranes. A brief account of some of the artificial membrane data has been published previously (Mellor et al. 1993).

Abbreviations: NODLN, Nodularin; MCYST-LR, Microcystin-LR; ADDA, 3-amino-9-methoxy-2,6,8-trimethyl-10-phenyldeca-4,6-dienoic acid; DPhL, diphytanoyl lecithin

Correspondence to: A. G. Petrov

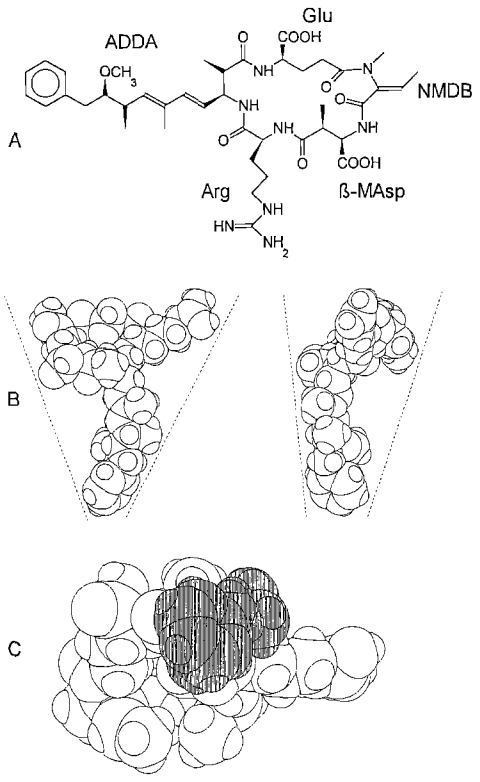

Fig. 1. **A** 2-dimensional representation of the structure of nodularin (NMDB = *N*-methyl-dehydrobutyrine, β-MAsp = β-methylaspartic acid, Arg = arginine, ADDA = 3-amino-9-methoxy-2,6,8-trimethyl-10-phenyldeca-4,6-dienoic acid, Glu = glutamic acid). **B** A 2-dimensional structure was prepared observing the configurations of all of the chiral carbons (as in Fig. 1 A). The 2-D structure was translated to 3-D using Quanta molecular modelling software and then 50 steps of steepest descents energy minimization were carried out to give a local energy minimum. The two views shown are at right angles to each other and show the ADDA sidechain projected downwards. The dotted lines emphasize the wedge-like structure of nodularin. **C** A view along the ADDA sidechain (shaded) shows the difference in cross sectional area between this and the cyclic part of the molecule

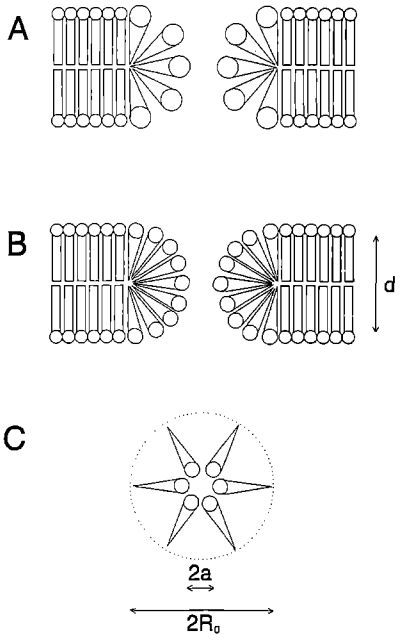

Fig. 2A–C. Aggregation of the toxin molecules into toroidal pores in a lipid bilayer according to their shape asymmetry. The steric asymmetry of NODLN **B** is less than that of MCYST-LR **A**. As such more NODLN monomers are required for formation of a pore. The tickness (d) of the hydrophobic core of the pore is identified. **C** Top view of a pore featuring the torus diameter ($2R_0$) and the narrowest part of the pore opening (2 a). The gaps between ADDA residues may be filled by adjacent lipid molecules below and above the narrowest cross-section of the open pore

2. Materials and methods

NODLN was purified from *Nodularia spumigena*. A natural bloom of this cyanobacterium was collected from the Barrow Water-Ski Club Lake, South Humberside, England, in June 1990. *N. spumigena* was grown in liquid Z8 medium (Kotai 1972) minus nitrate and containing 25% (v/v) filtered seawater. 8 L volumes of autoclaved, inoculated medium were incubated at 23 °C and sparged with filter-sterilized air at about 7 L per min. The cells were harvested by continuous centrifugation at 13 000 g (Sharples Limited). Cell pellets were lyophilized and stored at −20 °C for toxin extraction. For every gram of lyophilized *N. spumigena*, 100 ml of 5% (v/v) acetic acid were added and the mixture magnetically stirred for 15 min at room temperature. The extract was then centrifuged at 2500 g for 15 min and the supernatant decanted and retained. The pellet was re-extracted as before, the supernatant pooled and passed through a GF/C (Whatman) 7.0 cm filter disc. The filtrate was applied to a methanol-activated C_{18} environmental Sep-Pak cartridge (Waters Associates). After the cyanobacterial extract had been applied, the cartridge was washed with distilled water and eluted in a step-wise manner with increasing increments of 10% (v/v) methanol in distilled water. NODLN was recovered in the 40 and 50% methanol eluates, which were pooled and rotary-evaporated to dryness at 40 °C *in vacuo*. Toxin purification was by high performance liquid chromatography (HPLC). All HPLC equipment and columns were supplied by Waters (Division of Millipore). A gradient system consisting of two 510 pumps, a variable detector set at 238 nm and a radial compressed module with a 4 µm C_{18} Radial-Pak cartridge (Nova-Pak, 10 cm × 5 cm) were used. The mobile phases were: (A) Milli-Q water plus 0.05% (v/v) trifluoroacetic acid (TFA) and (B) acetonitrile plus 0.05% TFA. Solvent B was increased linearly from 25% to 50% over 25 min at a flow rate of 1 ml per min. The NODLN peak was collected and rotary evaporated to dryness, as before. For the biophysical studies reported herein, NODLN was re-dissolved in high-grade methanol (Fisons) at 200 µg/ml or lower.

Lipid bilayers were formed from diphytanoyl lecithin (DPhL) (M.W. 846.27, Avanti Polar Lipids, Birmingham, Alabama). The electrolyte was 150 mM KCl plus 1 mM TRIS, pH 7.2. Lipid bilayers were formed at the tip of patch pipettes, by the pipette dipping method of Coronado

and Latorre (1983), from lipid monolayers spread at an air/water interface. A solution of DPhL in *n*-hexane or in *n*-pentane (HPLC grade), typically at a concentration of 3 mg/ml, was employed. Patch pipettes were pulled from thick-walled borosilicate glass (GC 150-10, Clark Electromedical Instruments) on a modified vertical puller (IF Shokai Model IMP). Pipettes with tip diameters of about 2 μm were used. 10 cm^2 disposable Petri dishes were filled with 5 ml of buffer. 5–10 μl of lipid solution was spread onto the surface of the buffer from a micropipette. In these studies with artificial membranes, NODLN was placed in the Petri dish buffer to give a final concentration of 4–400 ng/ml.

Locust muscle membrane patches were excised from the surface membranes of metathoracic extensor tibiae muscle fibres of adult female locusts (*Schistocerca gregaria*), 7–10 days post-fledging (Huddie et al. 1986). The muscle was pretreated with collagenase (Sigma 1 A, 1.7 mg/ml) for 100 min at room temperature (20–22 °C) before patch formation. Patch pipettes and muscle bath contained standard locust saline (180 mM NaCl, 10 mM KCl, 2 mM $CaCl_2$, 10 mM HEPES, pH 6.8). For all experiments on locust muscles, pipettes were pulled and fire-polished on a DMZ-puller and coated with SYLGARD® resin. Pipette resistances were typically 8 MΩ. NODLN was added to the pipette saline at concentrations of 4–100 ng/ml. In some experiments patches were held at a pipette potential (V_{pip}) of −70 mV (which possibly assisted toxin emplacement because of the negative charge on the toxin). Patch currents were measured continuously to record the appearance of the first NODLN-induced pores and then breakdown of the patches. In other experiments, the membrane potential (V_{pip}) was ramped (duration 8–10 s) repeatedly between −40 mV and 40 mV.

The surface pressures of control lipid monolayers and of those exposed to NODLN were studied using a Wilhelmy-type surface tensiometer (Nima Technology Ltd., Model ST9000). The output of the tensiometer was sampled by a PC/AT computer as a function of time. In experiments on bilayers, constant pressures and pressure ramps were generated by a reversible peristaltic pump and monitored by a pressure meter using a MPX 100 AP (Motorola) silicon piezoresistive pressure sensor with an output of 1 mV/torr. Membrane currents were monitored using a home-made patch-clamp amplifier, with current and voltage outputs linked to an A/D convertor and recorded on the hard disc of a PC/AT Pravetz 16 Computer. Data analyses were undertaken using the Strathclyde Electrophysiological Software (Dempster 1993) and with modified current-voltage surface software (Sansom and Mellor 1990). One modification of the latter permitted the display of various sequences (linear, exponential, logarithmic etc.) of event number levels i.e. horizontal sections of current-voltage surfaces; another provided the possibility of displaying vertical sections of current-voltage surfaces at any chosen value of the voltage (or pressure) in the form of current amplitude histograms. Membrane potentials by convention bear the sign of the electrode inside the pipette. The same convention is adopted for the pressure (i.e. positive if the pressure was higher inside the pipette than outside).

3. Results

3.1. NODLN is a weak surfactant

The surface activity of NODLN was investigated at an air/water interface following addition of toxin to buffer. When the toxin concentration in the buffer was progressively increased to 400 ng/ml the surface pressure of the monolayer increased to 9.1 mN/m (Fig. 3). This result contrasts with that for MCYST-LR, for which a surface pressure of only 2.5 mN/m was obtained with 2 μg/ml MCYST-LR (Petrov et al. 1991). The solvent effect alone was negligible; the above mentioned NODLN increment was obtained by a total of 10 μl MeOH solution while 30 μl pure MeOH in 5 ml of buffer resulted in a surface pressure change of less then 0.3 mN/m. NODLN was also added to buffers supporting monolayers of DPhL of different surface pressures. In one example, the surface pressure in the absence of toxin was 13 mN/m. Addition of 20 μl of a 20 μg/ml NODLN solution to 5 ml of buffer (80 ng/ml) caused an increase in surface pressure of 1 mN/m. The surface pressure changed almost immediately (< 1 s) after the addition of the toxin. Solvent influence was negligible, i.e. surface pressure increases of < 0.1 mN/m were recorded when the same amount of pure MeOH was added to the buffer. The effect of toxin on surface pressure depended nonlinearly on the initial surface pressure of the monolayer, with the relationship exhibiting a maximum at about 22 mN/m and becoming negative at higher pressures (Fig. 4).

3.2. NODLN pores in lipid bilayers

NODLN pores were observed in 73 out of 147 bilayers. 65% of bilayers formed from monolayers exposed to toxin contained pores, whereas pores were observed in 43% of bilayers which were first formed and then exposed to toxin. Pores were observed almost immediately after bilayer formation in the former case, whereas in the latter case pore formation did not occur for 5–30 min. In both cases, pore formation was usually enhanced at positive V_{pip}.

In Fig. 5 A, where NODLN was added to a bilayer, pores were observed at + 60 mV and zero transmembrane pressure. The recording exhibits multiple conductance levels ranging between 100 pS and 2 nS (Fig. 5 B), with a conductance level of 416 pS having the highest probability of occurrence. Jumps in conductance were not always to consecutive levels (Fig. 5 A) suggesting that the conductances were for a single pore rather than for several pores. The finding that each of the conductance levels can be fitted by a single Gaussian distribution and that there are no shoulders corresponding to a 107 pS conductance supports this observation. The analysis of conductance level probabilities illustrated in Fig. 6 lends further support to this possibility (see Discussion).

Voltage-current surfaces were used to investigate the voltage dependence of pore formation (Fig. 7). There was a tendency for a reduction in the probability of occurrence of higher conductance states of the pore at higher voltages similar to the findings with MCYST-LR (Petrov et al. 1991).

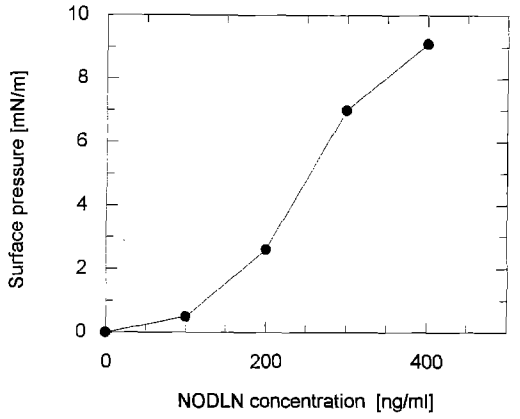

Fig. 3. The surface pressure of a pure NODLN monolayer as a function of NODLN concentration. A 200 μg/ml NODLN solution was added by successive 2.5 μl additions

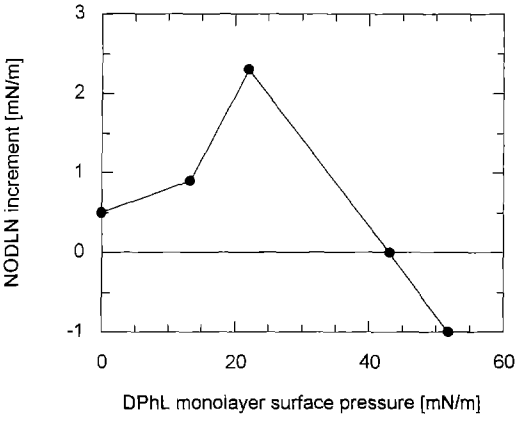

Fig. 4. The effect of NODLN on DPhL lipid monolayers with different surface pressures. NODLN was each time added to the subphase to give a final concentration of 80 ng/ml

3.3. Tension sensitivity of NODLN pores

The effect of transmembrane pressure on pore formation and conductance was studied by applying pressure steps from 0 torr to −50 torr, during the application of a voltage ramp of ±100 mV. Some typical results are shown in Fig. 8 A, B. Figure 8 A shows that higher conductance states at 0 torr are most probable in a narrower voltage range of ±50 mV around zero (cf. Fig. 7). Figure 8 B demonstrates the appearance of higher conductance states during −10 torr pressure application extending over the whole ±100 mV voltage range, while the closed and the lowest open state are completely suppressed. Although pores did not arise in another bilayer before pressure was applied, even with a voltage ramp of ±300 mV, a positive pressure of 45 torr resulted in the appearance of pores at $V_{pip} > \pm 120$ mV. Figure 9 demonstrates the effect of pressure on the averaged current through a toxin-containing bilayer. Application of −5 torr to the patch pipette lead to strong increase of current due to the appearance of a pore or pores of high conductance.

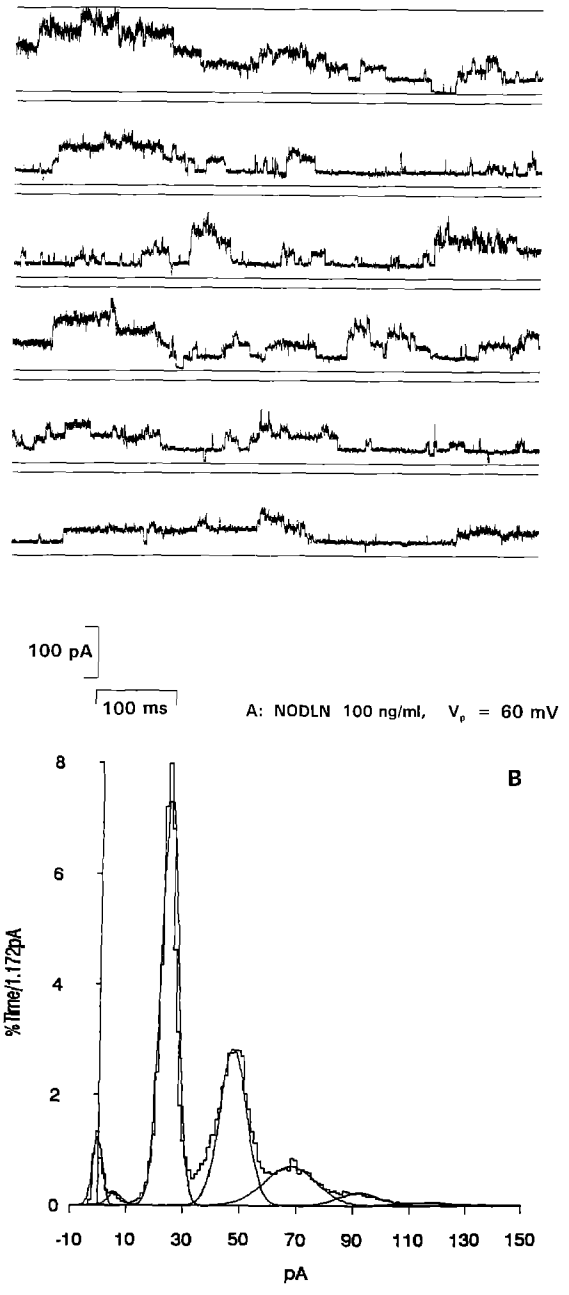

Fig. 5 A, B. Multiple conductance levels of a pore induced by NODLN in a lipid bilayer. NODLN was added to the buffer to give a final concentration of 100 ng/ml. V_{pip} was 60 mV. **A** A 4 s recording from the bilayer. Sampling rate was 10 KHz. **B** Amplitude histogram of the membrane current. The fitted levels are 0.0 pA, 6.40 pA, 24.96 pA, 48.08 pA, 68.32 pA, 92.80 pA, 117.90 pA and the probabilities are 0.05, 0.012, 0.48, 0.28, 0.14, 0.04, 0.01, respectively

The effect of pressure on pore formation at constant membrane potential was also studied. For example, in a membrane exhibiting no pores at zero pressure and V_{pip} of 200 mV, when the pressure was raised to −25 torr (at a rate of 0.1 torr/s) a pore of 30 pS conductance appeared at −3 torr. At −10 torr, conductances of 50–100 pS appeared and at −15 to −25 torr 400 pS pores were observed. These experiments were usually terminated by the membrane rupturing.

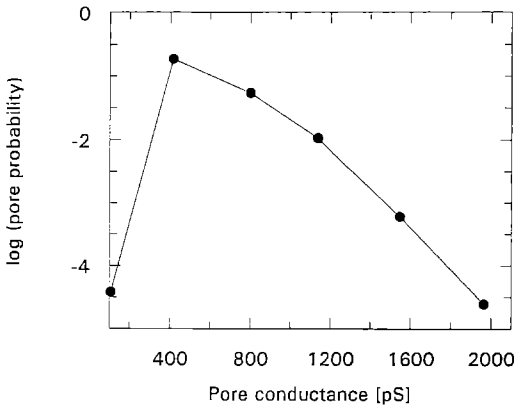

Fig. 6. Semi-log plot of the open state probabilities for the conductance levels observed in the recording illustrated in Fig. 5A as a function of pore conductance

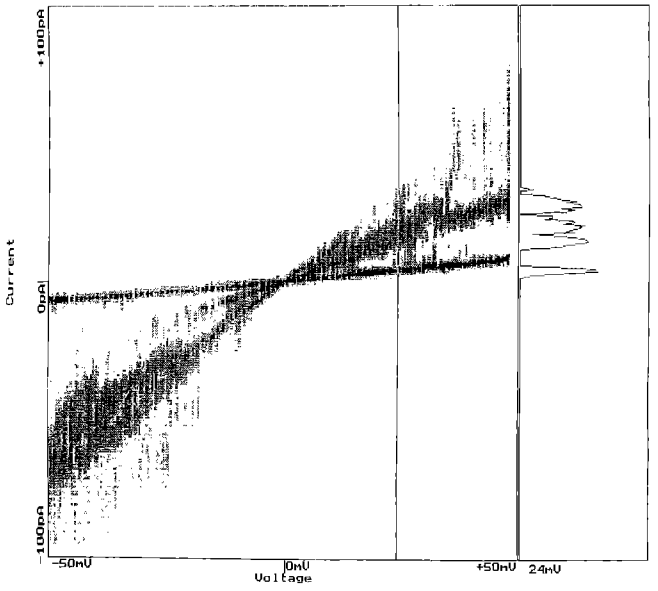

Fig. 7. Voltage-dependence of pore conductance. Current-voltage surface for a recording obtained at zero transmembrane pressure from a bilayer exposed to 100 ng/ml NODLN. The surface is an average of 4 voltage ramps of ±50 mV with a ramping rate of 1 mV/sec. Total duration of the record is 400 s. The inset on the right displays a vertical cross-section of the I-V surface at 24 mV (cursor line) in the form of a *log* current histogram. At positive potentials conductances of 468 pS, 702 pS and 1150 pS were identified

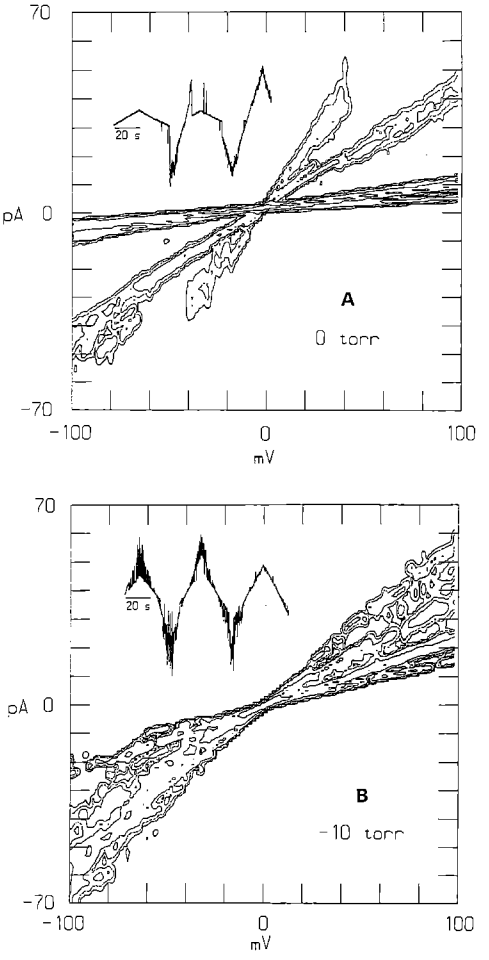

Fig. 8A, B. Current-voltage surfaces from a DPhL bilayer at 0 torr **A** and −10 torr **B**, exposed to 200 ng/ml NODLN. Insets: examples of raw current data for a ±100 mV voltage ramp (ramp rate 8 mV/s). Total duration of the record was 300 s. **A** Closed state and open conductance states of 54 pS, 420 pS and 915 pS (limited extent) were identified; **B** No closed state and extended open states of 113 pS, 183 pS, 323 pS, and 522 pS were identified

3.4. NODLN *pores in patches of locust muscle membrane*

In the absence of toxin, patches of locust muscle membrane displayed their familiar K^+-channel activity (Huddie et al. 1986; Gorczynska et al. 1994)). Their life-span was usually more than 30 min when V_{pip} was held at −50 to 50 mV. For our experiments we have selected, as a rule, patches which did not contain any natural K^+-channels to avoid confusion. When patches were exposed to toxin (up to 200 ng/ml in the pipette-filling normal locust saline), a reduction in their survivability was observed. With 100 ng/ml toxin (as in bilayer experiments) large pores of typically 250 pS conductance were observed, mainly with negative V_{pip} (not shown). These pores usually persisted in the open state and quickly grew in size until patch breakdown took place (usually within some 150 s). Locust patches proved more sensitive to NODLN than lipid bilayers. Figure 10A demonstrates the current trace of a locust muscle patch exposed to a lower NODLN concentration (20 ng/ml). A 35 pS pore appeared after 23 s and there was a further increase in conductance up to 90 pS at 123 s. In the time interval between 240 s and 320 s fluctuating behaviour of the pores was observed (Fig. 10B), quite similar to the bilayer case (Fig. 5A). At this concentration patches survived for about 400 s. The survivability of a patch was inversely related to toxin concentration. For example, with 4 ng/ml toxin, the time to patch breakdown was 600–700 s. Patches not exposed to toxin survived for about 800 s when held at the same V_{pip} of −70 mV. On the

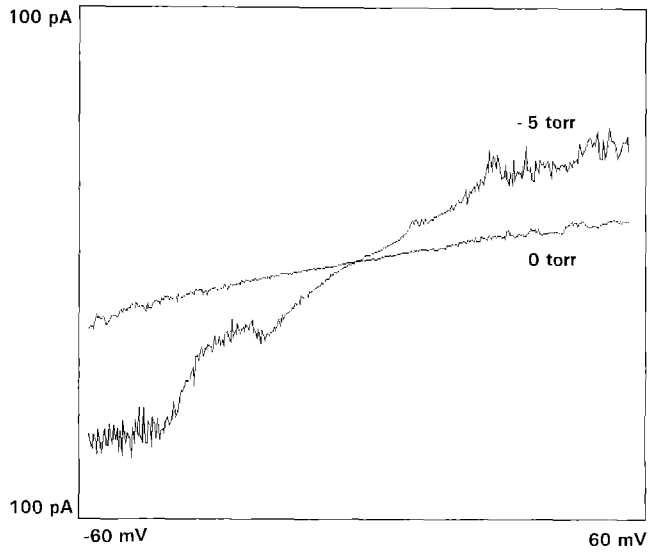

Fig. 9. Pressure dependence of the average pore current in response to a ±60 mV voltage ramp (12 mV/s), at 0 torr and −5 torr. NODLN concentration was 50 ng/ml. Total duration of each record was 60 s, averaged over 3 ramps

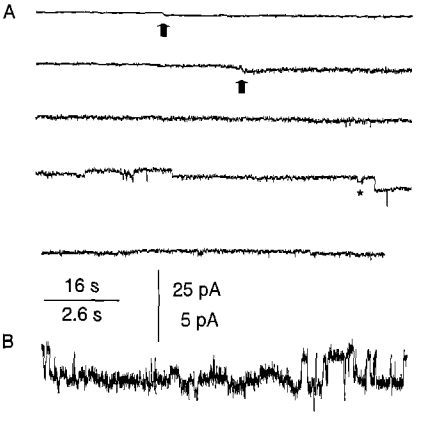

Fig. 10 A, B. Inside-out patch of locust muscle membrane. Pipette resistance was 9 MΩ, seal resistance was 27 GΩ. NODLN concentration in the pipette was 20 ng/ml. V_{pip} was −70 mV. **A** The first (35 pS) and second (90 pS) toxin-induced conductance increases are marked by arrows. Following the appearance of further conductance increases the patch broke down after 396 s. **B** An expanded part of the trace (marked by asterisk on **A**) showing in more detail openings and closings of toxin-induced pores

other hand patches exposed to even higher concentrations of toxin, but which were clamped at 0 mV, did not exhibit pores and survived for as long as control patches.

Survivability of a patch in voltage ramp experiments was longer than that for constant V_{pip} of the same amplitude but also inversely related to toxin concentration (not shown). The time interval between the first ramp and the appearance of a pore decreased by about 20-fold when the toxin concentration was increased by 50-fold (from 4 to 200 ng/ml). The I-V curve of the pores was essentially linear.

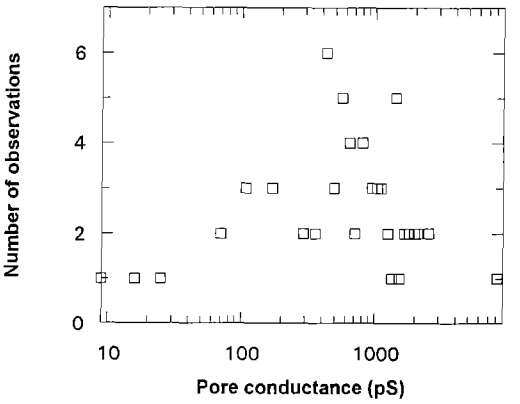

Fig. 11. Semi-log scattergram of NODLN-induced conductances in DPhL bilayers observed in 73 experiments with various toxin concentrations, voltages and pressures. 26 discrete conductance levels were identified

Typical pore conductances in the locust membrane patch experiments were 30 pS, 60 pS, 90 pS, 125 pS, 250 pS, 750 pS; i.e. similar to those found in lipid bilayers exposed to NODLN (cf. Fig. 11). However, unlike the pores observed with bilayers, the pores in locust membrane patches were metastable, i.e. they mostly stayed open and rarely exhibit transient closings. Also, locust membrane sensitivity to this toxin was higher, i.e. lower NODLN concentrations than in model experiments were still effective in porating living membranes.

4. Discussion

The results of these studies indicate that NODLN interaction with a DPhL monolayer is accompanied by reorganisation of the lipid molecules comprising the monolayer. The lipid density corresponding to 22 mN/m lateral pressure might cause a maximal shift of the NODLN partition coefficient $[N_w]/[N_s]$, where $[N_w]$ in NODLN concentration in the solution and $[N_s]$ is NODLN surface concentration. Let us note that the lateral pressure of biological membranes is about 25 mN/m (e.g. Israelachvili et al. 1980). Therefore, an optimal partitioning of the toxin could be expected when in contact with a native membrane, as actually observed with the locust muscle membrane. The reduction in surface pressure that was obtained during toxin application to high density monolayers (Fig. 4) could be due to the removal of lipid molecules from the monolayer through the formation of pre-micellar toxin/lipid aggregates. Differences in the biphilic asymmetries of NODLN and MCYST-LR might account for the observed differences in their surface activities. This suggests that under optimal conditions the buffer concentration of NODLN sufficient to produce membrane pores could, perhaps, be lower than that for MCYST-LR. Indeed, in separate experiments with (larger area) Montal-Mueller membranes, and with locust membranes, pore activity was observed with 4 ng/ml toxin.

The NODLN-induced conductances observed in lipid bilayers are summarized in Fig. 11 in the form of a scattergram. The conductances ranged from 9 pS to 8.2 nS. In some bilayers a single pore with different conductance states seemed to be present, but in others it was possible that more than one pore was present. In the former case, the discreteness of the conductance levels could be due to changes in the number of molecules in the pore perimeter.

It was shown by Petrov et al. (1980) that in a tension-free membrane a toroidal pore with a curved monolayer edge (Fig. 2) will feature a local minimum free elastic energy W_0 at a specific pore radius R_0 corresponding to a metastable open state. The occupation probability P_i of a conductance state of energy W_i will be (e.g. Sugar 1989):

$$P_i = A \exp(-W_i/k_B T), \quad (1)$$

where k_B is Boltzmann constant and T is absolute temperature. Therefore, the minimum energy state (W_0) will be most probable. Other conductance states could also occur, but with lower probabilities.

If a lipid bilayer or a native membrane patch, located at the tip of a patch pipette, is subjected to a transmembrane pressure difference (Δp), the lateral tension (σ_0) of the membrane will increase. The adhesion model of Opsahl and Webb (1994b), combined with the Laplace Law yields the following expression for σ_0:

$$\sigma_0 = \sigma_a(1 + r_p^2 \Delta p^2 / 4\sigma_a^2)^{1/2}, \quad (2)$$

where σ_a is the membrane-glass adhesion energy (it is also the initial membrane tension) and r_p is the patch radius. Petrov et al. (1991) have shown how σ_0 increases the zero-tension radius (R_0) of a metastable toroidal pore (Fig. 2C). Equation (3) demonstrates that transmembrane pressure will enhance pore opening (cf. Figs. 8 and 9). The effects of transmembrane electric field on pore diameter can be considered within the same theoretical framework if a ponderomotive, voltage-dependent lateral tension is introduced. The edge energy γ_0 of a pore might also be voltage dependent (Petrov et al. 1980).

Pores formed in lipid bilayers by α-helical polypeptides, such as alamethicin, have been described in terms of a barrel-stave model (e.g. Inouye 1974; Mellor et al. 1988; Sansom 1991), which provides a simple expression for the pore conductance (g) in terms of the pore radius (a) and length (l):

$$g = \pi a^2 \kappa / (l + \pi a/2), \quad (3)$$

where κ is the specific conductivity of electrolyte filling the pore. This expression could also be applied to toroidal pores, if it is assumed that 2a is the narrowest opening of the torus (Fig. 2C). Since the pore energy increases quadratically around a minimum as the pore radius increases (Petrov et al. 1980), it might be anticipated that the log of the probabilities of higher energy states (From Eq. (1)) will decrease linearly as the pore conductance (g_i) increases:

$$\log_e P_i = -(8\gamma_0/\kappa k_B T) g_i + \text{const}, \quad (4)$$

where γ_0 is the specific edge energy per unit length of the pore perimeter. Equation (4) is derived under the assumption that the minimum energy state has a radius R_0 close to $l/2$, where l is the bilayer thickness (in Eq. (3)), and has therefore a low conductance. Figure 6 yields a slope of $\log_e P_i$ vs g_i dependence of 2.5×10^{-3} $(pS)^{-1}$. Consequently, with $\kappa = 1.1$ S/m (Robinson and Stokes 1965) a value of the edge energy of a NODLN pore of

$$\gamma_0 = 1.4 \times 10^{-12} \text{ J/m} \quad (5)$$

is calculated. Comparing this value to the earlier measured edge energy of pure egg lecithin ($\gamma_0 = 2.1 \times 10^{-11}$ J/m, Harbich and Helfrich 1979) we see how wedge-like NODLN molecules decrease the edge energy of the lecithin matrix and in this way increase strongly the probability of pore nucleation. This is in accordance with the theory of Petrov et al. (1980).

Table 1. Theoretical calculation and experimental data for the conductance levels of a NODLN pore. The theoretical calculation was based on Eq. (3) in the text, considering the pore as a cylinder. The pore length l was taken equal to the capacitive thickness d of a solvent-free bilayer from saturated C_{16} alkyl chains of lecithin, i.e. 2.4 nm (this value was obtained by extrapolation of the measured values by Benz et al. (1975) down to C_{16} chain length). Pore radius a was calculated from $a = Nn/2\pi$, where Nn is the length of the pore perimeter, N is the number of toxin molecules in the pore perimeter and n = 0.77 nM is the linear dimension of the hydrophilic head of the NODLN molecule which corresponds to the minimum energy molecular conformation (Fig. 1B). Specific conductivity $\kappa = 1.1$ S/m for 0.1 M KCl solution was taken from Appendix 5.1 of Robinson and Stokes (1965). The successive levels were calculated for increasing pore perimeters in steps (N) by 2 additional toxin molecules

N	g (theory) [pS]	g (experiment) [pS]
4	262	107
6	525	416
8	843	801
10	1200	1139
12	1587	1547
14	1997	1965

Theoretical calculations of pore conductances in terms of a barrel-stave model of a single pore are compared to the experimental values in Table 1. It is clear that some of the theoretical values for pore conductances based on the barrel-stave model match some of the conductance levels obtained in the bilayer studies with NODLN when only one pore appeared to be present in a bilayer. The differences between the conductance states in Table 1 are close to theoretical values based on differences in the size of a NODLN pore, i.e. the increase of conductivity which might be expected by recruiting a pair of molecules to the narrowest place of the pore. Perhaps a pore structure containing an even number of peripheral molecules is more favourable than an odd number one, with the hexamer being the most favourable. The agreement between theory and experiment becomes better at higher pore radii. For narrower pores, the pore opening is smaller than the circle passing through the middle of toxin head groups, also the pore cross section is far from cylindrical. In fact, pores with conductances less than 100 pS probably have different structures from that postulated in Fig. 2. Finally, the relationship between the electrolyte conductivity in a pore

is not the same for narrow and wide pores (e.g. Pastushenko and Petrov 1984).

The effect of σ_0 on the switching of alamethicin pores between open channel conductance states was reported recently (Opsahl and Webb 1994 a). A gating mechanical energy in the form

$$W_{ji} = \sigma_0 \Delta A_{ji}, \quad (6)$$

where $\Delta A_{ji} = A_j - A_i$ is the gating area, i.e. the area difference between j and i state of the pore was employed to describe the tension dependence of occupation probabilities of the states i and j. This approach could also be applied to NODLN pores; however it requires optical monitoring of the patch geometry in order to determine the parameters in Eq. (2).

The ability of NODLN to porate a natural membrane is revealed here for the first time. Hitherto, the toxicity of hepatotoxins from cyanobacteria has been considered to arise from the inhibition of protein phosphatases (Honkanen et al. 1990; MacKintosh et al. 1990; Yoshizawa et al. 1990; Falconer and Yeung 1992). The results described herein suggest that a direct action on cell membranes may also be involved in toxicity.

Acknowledgements. This work was supported by a British Council Academic Link between the Institute of Solid State Physics, Sofia and Nottingham University, by an EC grant to PNRU (No 3911) and by the Bulgarian National Fund "Scientific Studies" (Project F 19). Thanks are due to Dr. R. L. Ramsey for the gift of a patch-clamp amplifier, to Dr. J. Dempster for supplying AGP with Strathclyde Electrophysiological Software and to Mr I. Bonev for help with the current-voltage software.

References

Benz R, Fröhlich O, Läuger P, Montal M (1975) Electrical capacity of black lipid films and of lipid bilayers made from monolayers. Biochim Biophys Acta 394:323–334

Carmichael WW (1989) Freshwater cyanobacteria (blue-green algae) toxins. In: Ownby CL, Odell GV (eds) Natural toxins. Characterization, pharmacology and therapeutics. Pergamon Press, Oxford, pp 3–16

Corronado R, Latorre R (1983) Phospholipid bilayers made from monolayers on patch-clamp pipettes. Biophys J 43:231–236

Dempster J (1993) Computer analysis of electrophysiological signals. Academic Press, London

Derzhanski A, Petrov AG (1982) Multipole model of the molecular asymmetry in thermotropic and lyotropic liquid crystals. Mol Cryst Liq Cryst 89:339–360

Falconer IR, Yeung DSK (1992) Cytoskeletal changes in hepatocytes induced by *Microcystis* toxins and their relation to hyperphosphorylation of cell proteins. Chem-Biol Interact 81:181–196

Gorczynska E, Huddie P, Mellor I, Miller BA, Ramsey RL, Usherwood PNR, Vais H (1994) Potassium channels of adult locust muscle. (In preparation)

Harbich W, Helfrich W (1979) Alignment and opening of giant lecithin vesicles by electric field. Z Naturforsch 34a:1063–1065

Honkanen RE, Zwiller J, Moore RE, Daily SL, Khatra BS, Dukelow M, Boynton AL (1990) Characterization of microcystin-LR, a potent inhibitor of type 1 and type 2 A protein phosphatases. J Biol Chem 265:19401–19404

Huddie PL, Ramsey RL, Usherwood PNR (1986) Single potassium channels of adult locust (*Schistocerca gregaria*) muscle recorded using the giga-ohm seal patch-clamp technique. J Physiol 378:60 P

Inouye M (1974) A three-dimensional molecular assembly model of a lipoprotein from the *Escherichia coli* outer membrane. Proc Natl Acad Sci USA 71:2396–2400

Israelachvili J, Marcelja S, Horn RG (1980) Physical principles of membrane organization. Quart Rev Biophys 13:121–200

Kotai J (1972) Instructions for preparation of modified nutrient solution Z8 for algae. Norwegian Institute for water research B 11/69. Blindern, Oslo

MacKintosh C, Beattie KA, Klumpp S, Cohen P, Codd GA (1990) Cyanobacterial microcystin-LR is a potent and specific inhibitor of protein phosphatases 1 and 2 A from both mammals and higher plants. FEBS Lett 264:187–192

Mellor I, Thomas DH, Sansom MSP (1988) Properties of ion channels formed by *Staphylococcus aureus* δ-toxin. Biochim Biophys Acta 942:280–294

Mellor I, Usherwood PNR, Codd GA, Petrov AG (1993) Nodularin, a cyclic pentameric peptide, forms ion channels in lipid bilayers. C R Acad Bulg Sci 46:53–55

Opsahl LR, Webb WW (1994 a) Transduction of membrane tension by the ion channel alamethicin. Biophys J 66:71–74

Opsahl LR, Webb WW (1994 b) Lipid-glass adhesion in giga-sealed patch-clamped membranes. Biophys J 66:75–79

Pastushenko VF, Petrov AG (1984) Electromechanical mechanism of pore formation in bilayer lipid membranes. Seventh School Biophys. Membrane Transport, Poland, School Proceedings, Wroclaw, vol 2, pp 69–91

Petrov AG (1988) Generalized lipid asymmetry and instability phenomena in membranes. Ninth School on Biophysics of Membrane Transport. School Proceedings, Wroclaw, Poland, vol 2, pp 67–86

Petrov AG, Derzhanski A (1987) Generalized asymmetry of thermotropic and lyotropic mesogens. Mol Cryst Liq Cryst 151: 303–333

Petrov AG, Mitov MD, Derzhanski A (1980) Edge energy and pore stability in bilayer lipid membranes. In Bata L (ed) Advances in liquid crystal research and applications. Pergamon Press, Oxford, pp 695–737

Petrov AG, Ramsey RL, Codd GA, Usherwood PNR (1991) Modelling mechanosensitivity in membranes: effects of lateral tension on ionic pores in a microcystin toxin-containing membrane. Eur Biophys J 20:17–29

Robinson RA, Stokes RH (1965) Electrolyte solutions, 2nd edn. Butterworths, London, p 462

Sansom MSP (1991) The biophysics of peptide models of ion channels. Prog Biophys Mol Biol 55:139–235

Sansom MSP, Mellor IR (1990) Analysis of the gating of single ion channels using current-voltage surfaces. J theor Biol 114: 213–223

Sugar IP (1989) Stochastic model of electric field-induced membrane pores. In: Neumann E, Sowers AE, Jordan CA (eds) Electroporation and electrofusion in cell biology, Plenum Press, New York London, pp 97–110

Yoshizawa S, Matsushima R, Watanabe MF, Harada K-I, Ichihara A, Carmichael WW, Fujiki H (1990) Inhibition of protein phosphatases by microcystin and nodularin associated with hepatotoxicity. J Cancer Res Clin Oncol 116:609–614